High-Density Polyethylene/Cycloolefin Copolymer Blends. Part 1: Phase Structure, Dynamic Mechanical, Tensile, and Impact Properties

J. Kolařík, Z. Kruliš, M. Šlouf
Institute of Macromolecular Chemistry, Academy of Sciences of the Czech Republic, 162 06 Prague 6, Czech Republic

L. Fambri
Department of Materials Engineering and Industrial Technologies, University of Trento, 38050 Trento, Italy

High-density polyethylene (HDPE) was blended with "reinforcing" cycloolefin copolymer (COC) in order to produce polyolefin materials with increased stiffness, yield and tensile strength. Experimental data on tensile modulus E_b, creep modulus E_{bcr}, storage modulus E_b', loss modulus E_b'', yield strength S_{yb}, and tensile strength S_{ub} of blends are in plausible accord with their simultaneous prediction based on a predictive format that operates with a two-parameter equivalent box model and the data on the phase continuity of components obtained from modified equations of the percolation theory. Dependencies of these mechanical properties on blend composition indicate the critical volume fraction $v_{2cr} = 0.16$ of COC. Interfacial adhesion in the HDPE/COC blends is strong enough to transmit acting stress up to the break point. Strain at break, tensile energy to break and tensile impact strength show conspicuous drops in the interval 15–25% of COC in the blends, during which COC starts to form a co-continuous brittle component. Further growth of COC fraction accounts for reduction of blend ultimate properties to values typical of brittle polymers. However, tensile impact strength shows a local maximum at HDPE/COC = 25/75, which probably corresponds to COC toughened with HDPE particles. POLYM. ENG. SCI., 45:817–826, 2005. © 2005 Society of Plastics Engineers

INTRODUCTION

Polyethylene (PE) shows a relatively low yield strength and a high propensity to creeping. These deficiencies can be alleviated by blending PE with a yield- and/or creep-resistant polymer, which forms a co-continuous blend component. In general, preparation of such PE blends may be rather difficult because the compatibility of the polymers is usually rather limited [1−5]. Attainment of satisfactory mechanical properties of blends frequently depends on finding a suitable compatibilizer that allows for sufficient interfacial adhesion, finer phase structure, lower tendency to phase structure coarsening, etc. Thus, search for "reinforcing" components imparting better mechanical properties to PE matrices remains an urgent problem.

Amorphous ethylene-norbornene copolymers obtained with metallocene-based catalysts [6−8] rank among new polymeric materials with remarkable properties, such as a relatively high glass transition temperature (T_g), heat resistance, chemical resistance to common solvents, low moisture uptake, high water barrier, and good mechanical properties. Available products—usually denoted as cycloolefin copolymers (COC)—have recently attracted much attention in the field of materials science [9−14]. Studies of mechanical properties of COC encompass dynamic mechanical thermal analysis (DMTA) [12, 14], stress-strain measurements [6, 11], flexural creep [6], microhardness [12], impact strength [9], etc. Rising percentage of norbornene accounts for increase in yield or tensile strength and decrease in strain at yielding and break [6, 11]. Because of a high fraction of ethylene units, COC is likely [15, 16] to be compatible with polyethylene and other polyolefins [17−19] without addition of special compatibilizers. Of available COC products of Ticona [6] we used Topas 8007, i.e., the copolymer with only 30% of norbornene, which displays yielding and breaks at about 10% of strain. We intended to prepare blends with a co-continuous reinforcing component to enhance modulus, yield strength, resistance to creep, etc. [20−24]. Searching for the critical volume fraction of COC, at which this component assumes partial continuity in

Correspondence to: J. Kolařík; e-mail: kolarik@imc.cas.cz
Contract grant sponsor: Grant Agency of the Czech Republic; contract grant numbers: 106/04/1051 (to J.K.), 106/02/P029 (to M.Š.).
DOI 10.1002/pen.20337
Published online in Wiley InterScience (www.interscience.wiley.com).
© 2005 Society of Plastics Engineers

blends with PE, our interest was mainly focused on the composition interval up to 50% COC.

From a practical point of view, it is desirable to have means for anticipating at least some of the considered properties of intended blends as functions of blend composition. At present, various models exist that predict individual properties of composite systems consisting of a continuous matrix and one or more dispersed (discontinuous) components [25]. Such models could be applied to polymer blends merely in the marginal composition intervals in which the minority component is fully discontinuous. Numerous studies [26−31] have shown that the minority component in two-component heterogeneous blends assumes partial continuity at the critical volume fraction v_{cr}, which is usually located in the interval $0.15 < v_{cr} < 0.3$. In the central composition interval between the critical volume fraction v_{1cr} and v_{2cr} of the constituents, phase structures with partially co-continuous constituents are typical of polymer blends. In our previous papers [18, 27, 29, 32−36], we have proposed a predictive scheme for modulus E_b, time-dependent compliance $D_b(t)$, yield strength S_{yb} (or tensile strength S_{ub}) and permeability P_b of polymer blends. The objective of this article is to ascertain the effects of the transition from a solely particulate phase structure to partly co-continuous phase structure on dynamic mechanical, tensile and impact properties of the PE/COC blends and compare them, wherever possible, with model predictions.

EXPERIMENTAL

Materials

A high-density polyethylene (HDPE), Liten BB 29 (Chemopetrol, Litvínov, Czech Republic), is characterized by melt flow index (MFI) (230°C, 2.16 kg) = 1.15 g/10 min (ISO 1133); density (ISO 1183) 0.956 g/cm^3; weight-average molar mass M_w = 420,000.

An amorphous cycloolefin copolymer produced under the trade name Topas 8007 was a product of Ticona (Celanese, Germany), consisting of 30% of bicyclo[2.2.1]hept-2-ene (norbornene) units and 70% of ethylene units [6]: MFI (260°C, 2.16 kg) = 34.3 g/ 10 min; density: 1.014 g/cm^3; T_g = 81°C.

Blend Preparation

A series of HDPE/COC blends was prepared with 10, 15, 20, 25, 30, 40, 50, and 75 wt% of COC. As our intention was to prepare binary blends with co-continuous minority COC component, it was necessary to use COC of a lower relative viscosity (in comparison with that of HDPE) with regard to the generally known fact (26, 27, 30, 31) that the component with lower viscosity shows a lower percolation threshold. Polymers were mixed in the W50EHT mixer of a Brabender Plasti-Corder at 220°C and 60 rpm for 10 min. The initial ratio of the HDPE and COC torques at the processing temperature was about 23/6, which was favorable for the phase co-continuity of COC in blends. Compression molding (press Fontijne; initial temperature: 230°C; pressure 3.1 MPa applied for 2 min; cooling time to room temperature: approximately 20 min) was used to obtain plates 100 × 100 × 1.7 mm from which three types of test pieces were prepared: 1) strips (10 mm in width) were sawn for the measurements of dynamic mechanical properties and creep; 2) two types of dumb-bell specimens were machined for the measurements of stress-strain dependencies or tensile impact strength. Specimens used for the measurements of mechanical properties were stored for more than six months at room temperature to avoid any interfering effect of physical aging during measurements.

Electron Microscopy

Scanning electron microscopy (SEM) and scanning transmission electron microscopy (STEM) images were obtained with scanning electron microscopes JSM 6400 (Jeol, Japan) and Vega TS 5130 with a transmission adapter (Tescan, Czech Republic), respectively. SEM microphotographs were the secondary electron images taken at an acceleration voltage of 25 kV. STEM microphotographs were taken at an acceleration voltage of 30 kV. Fracture surfaces of the blends fractured in liquid nitrogen were sputtered with platinum for examination in SEM. Ultrathin sections for STEM were cut at −130°C (with an ultramicrotome equipped with a cryoattachment), washed, transferred to copper support grids and stained with RuO_4 vapors. The staining was based on the reaction of $RuCl_3 \cdot \times H_2O$ with NaOCl as described in the literature [37]; staining times were around 100 min. STEM microphotographs display PE as bright regions and COC as dark regions.

Differential Scanning Calorimetry

A Mettler differential scanning calorimeter (DSC) 30 was used to perform two consecutive heating scans in the interval 0 to 200°C. The heating rate and the cooling rate (between the scans) were 10°C/min. Tests were run under nitrogen atmosphere (flux: 100 ml/min). Test specimens (about 20 mg taken from the same position of compression molded plates) were used to ascertain the glass transition temperature T_{g2} of the COC component, the melting temperature T_{m1} and the melting enthalpy ΔH_{m1} of the HDPE component. The crystallinity (in %) of the HDPE in blends is given as $C_1 = 100\ w_1\ \Delta H_{m1}/\Delta H_{m1o}$, where w_1 is the weight fraction of HDPE in the blends and ΔH_{m1o} = 293.5 J/g is the melting enthalpy of the crystalline phase of PE [38].

Dynamic Mechanical Thermal Analysis

Dynamic mechanical thermal analysis (DMTA) measurements were performed with a DMTA Mk II (Polymer Laboratories Ltd, Loughborough, UK) operated in the sin-

15482634, 2005, 6, Downloaded from https://4spepublications.onlinelibrary.wiley.com/doi/10.1002/pen.20337 by Universita Di Trento, Wiley Online Library on [14/10/2026]. See the Terms and Conditions (https://onlinelibrary.wiley.com/terms-and-conditions) on Wiley Online Library for rules of use; OA articles are governed by the applicable Creative Commons License

gle cantilever bending mode with test specimens 12 × 10 × 1.7 mm. Storage E′ and loss E″ moduli were measured at frequency of 1 Hz in the range –140 to 120°C (heating rate 3°C/min; dynamic displacement 0.032 mm). To evaluate the coefficient of (linear) thermal expansion (CTE), tensile DMTA measurements were performed (specimens 18 × 10 × 1.7 mm; static stress: 0.19 MPa; dynamic displacement: 0.032 mm; heating rate: 3°C/min; temperature range: –20 to 90°C). CTE = $(\Delta L/L_0)/\Delta T$ was calculated for three different temperature intervals ΔT by using the initial specimen length L_0 and the length variation ΔL in the selected interval ΔT.

Stress-Strain Measurements

An Instron Tester, type 5800, was used to measure tensile mechanical properties on dog-bone shape specimens (gauge length: 50 mm; gauge cross-section: 10 × 1.7 mm) at a cross-head speed of 5 mm/min.

Tensile Creep Measurements

Tensile creep was measured at room temperature by using an apparatus equipped with a mechanical stress amplifier (lever) 10:1. The measurements at four stress levels were performed with one test specimen; each measurement was followed by a 22 h recovery before subsequent creep test (at a higher stress) was initiated. Specimen dimensions: initial distance between grips: 80 mm; cross-section: 10 × 1.7 mm. Creep modulus E_{cr}(1 min) corresponds to the inverted value of compliance after 1 min of creeping. In view of highly nonlinear stress-strain behavior of the PE/COC blends, E_{cr}(1 min) was interpolated for the strain 0.5% by using the data from four creep measurements at different stresses.

Tensile Impact Strength

Tensile impact strength (TIS) was measured at 23°C using a Zwick impact tester equipped with a special fixture for test specimens according to ISO 8256. For each material, 12 specimens were tested.

PREDICTIVE SCHEME

Polymer blends are isotropic materials with three-dimensional continuity of one or more components so that parallel or series models, models for orthotropic or quasi-isotropic materials, etc., are not applicable. Our predictive format [17, 18, 27, 32−36] is based on a combination of an equivalent box model (EBM) and modified equations rendered by the percolation theory for two-component systems [31, 39−41], which operates with the critical volume fractions v_{1cr} and v_{2cr} of constituents 1 and 2, respectively. The EBM in Fig. 1 consists of the fractions of components 1 and 2 coupled either in parallel (v_{1p} and v_{2p}) or in series (v_{1s} and v_{2s}). The blocks (fractions) in the EBM are presumed to have physical properties of the neat components; the application of the EBM is likely to fail if the mixing process produces a significant change in the structure and properties of a constituent. The EBM is a two-parameter model, because only two of its four volume fractions v_{ij} are independent; its volume fractions are interrelated as follows:

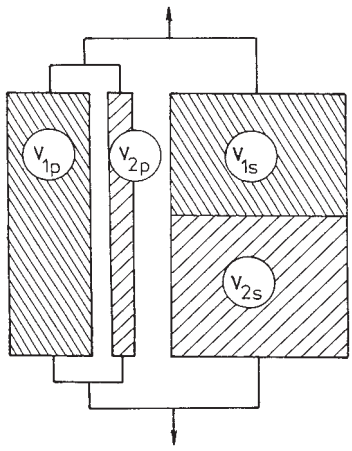


FIG. 1. Equivalent box model for a binary blend (schematically).

$$v_1 = v_{1p} + v_{1s}; \quad v_2 = v_{2p} + v_{2s}; \quad v_1 + v_2 = v_p + v_s = 1. \qquad (1)$$

As the EBMs are not self-consistent models, the predictive format requires two steps: 1) to derive the equations for the blend properties under consideration; and 2) to calculate the volume fractions v_{ij} by using another appropriate model. An essential feature of the predictive format is that all simultaneously predicted properties of a blend are related to a certain phase structure through an identical set of input parameters.

Equations for Moduli, Yield, and Tensile Strength of Binary Blends in Terms of the EBM

The resulting tensile modulus of a two-component system visualized in Fig. 1 is [32−34]:

$$E_b = E_1 v_{1p} + E_2 v_{2p} + v_s^2/[(v_{1s}/E_1) + (v_{2s}/E_2)] \qquad (2)$$

where $v_s = v_{1s} + v_{2s}$. Dynamic mechanical measurement at a constant frequency is the case of steady state harmonic conditions for which the elastic-viscoelastic correspondence principle is applicable [42]. Thus isochronous DMTA makes it possible to use the models derived for elastic materials also for viscoelastic materials by replacing elastic constants by their complex counterparts [32]. Introducing $E_1^* = E_1' + iE_1''$, $E_2^* = E_2' + iE_2''$ and $E_b^* = E_b' + iE_b''$ into *Eq. 2* and separating the real and imaginary terms, we obtain

$$E_b' = E_1' v_{1p} + E_2' v_{2p} + v_s^2 N'/D \qquad (3)$$

15482634, 2005, 6, Downloaded from https://4spepublications.onlinelibrary.wiley.com/doi/10.1002/pen.20337 by Universita Di Trento, Wiley Online Library on [14/10/2026]. See the Terms and Conditions (https://onlinelibrary.wiley.com/terms-and-conditions) on Wiley Online Library for rules of use; OA articles are governed by the applicable Creative Commons License

$$E''_b = E''_1 v_{1p} + E''_2 v_{2p} + v_s^2 N''/D \quad (4)$$

where

$$N' = v_{1s}E'_1(E'^2_2 + E''^2_2) + v_{2s}E'_2(E'^2_1 + E''^2_1) \quad (5a)$$

$$N'' = v_{1s}E''_1(E'^2_2 + E''^2_2) + v_{2s}E''_2(E'^2_1 + E''^2_1) \quad (5b)$$

$$D = (v_{1s}E'_2 + v_{2s}E'_1)^2 + (v_{1s}E''_2 + v_{2s}E''_1)^2. \quad (5c)$$

A linear stress-strain relationship indispensable for modulus measurements can be granted for glassy and/or crystalline constituents of blends only at very low strains, typically a few tenths of a percent, at which interfacial adhesion in the blends is usually sufficient for the transmission of applied low stresses. At higher strains (usually 3–6%), yielding and plastic deformation of blend components may occur. In our previous articles [32−34], we derived the equation for yield strength S_{yb}:

$$S_{yb} = S_{y1}v_{1p} + S_{y2}v_{2p} + AS_{y1}v_s, \quad (6)$$

where $S_{y1} < S_{y2}$ characterize the parent polymers and A the extent of interfacial debonding. Two limiting values of S_{yb}, viewed as the lower or upper bound, can be distinguished by means of *Eq. 6*: 1) The lower bound of S_{yb} is observed if interfacial adhesion is so weak that complete debonding occurs between the fractions of constituents coupled in series ($A = 0$ at S_{yb}). 2) The upper bound of S_{yb} is achieved if interfacial adhesion is strong enough to transmit the acting stress between constituents in the course of yielding so that no debonding appears ($A = 1$). However, if two components differing in the yield strength are coupled in series, then the branch yields at S_{y1} or S_{y2}, whichever is lower. With regard to the previous experience [25] that formally identical equations can be used for evaluation of the yield as well as tensile strength of particulate systems, we have also tentatively applied [33, 43] *Eq. 6* for S_{ub} by replacing the yield strengths S_{y1} and S_{y2} with the tensile strengths S_{u1} and S_{u2}, respectively.

Calculation of Input Parameters for EBM

The percolation theory [39−41] has provided a universal formula for the elastic modulus of binary systems in which the contribution of the second component is negligible. This formula has allowed us to derive [27, 33−35, 43] relatively simple equations for v_{1p} and v_{2p}:

$$v_{1p} = [(v_1 - v_{1cr})/(1 - v_{1cr})]^q, \quad (7a)$$

$$v_{2p} = [(v_2 - v_{2cr})/(1 - v_{2cr})]^q \quad (7b)$$

where v_{1cr} and v_{2cr} are the critical volume fraction (the percolation threshold) at which the components become partially continuous and q is the critical exponent. The remaining v_{1s} and v_{2s} are evaluated by using *Eq. 1*. In the marginal zone $0 < v_1 < v_{1cr}$ (or $0 < v_2 < v_{2cr}$), where only component 2 (or 1) is continuous, simplified relations can be used for the minority component, i.e., $v_{1p} = 0$, $v_{1s} = v_1$ (or $v_{2p} = 0$, $v_{2s} = v_2$), to obtain an approximate prediction of considered properties. Most ascertained values of q are located in an interval of 1.6–2.0 so that $q = 1.8$ can be used also as an average value in conformity with the theoretical value 11/6 [39]. For three-dimensional cubic lattice, the percolation threshold $v_{cr} = 0.156$ was calculated [30, 31, 40, 41]. In general, the patterns predicted by using "universal" values $v_{1cr} = v_{2cr} = 0.156$ and $q = 1.8$ should be viewed as a first approximation that may not be in a good accord with experimental data because real v_{1cr} and v_{2cr} of polymer blends frequently differ from 0.156 and from each other. Actual values of the parameters for a specific blend can be adjusted by fitting experimental data on physical properties of blends by *Eqs. 2*, *3*, *4*, and *6*.

RESULTS AND DISCUSSION

Phase Structure and Crystallinity of Blends

SEM microphotographs of fracture surfaces of the 85/15, 70/30, and 50/50 blends (Fig. 2) clearly distinguish between PE and COC. Although the fracture surfaces were prepared in liquid nitrogen, i.e., far below the T_g of blend components, the fracture surface of PE exhibits typical plastic deformations, which develop due to local overheating during the fracture [44]. Fracture surfaces of COC component are quite smooth because of its brittle fracture. Similar effects were previously observed in analogous PP/COC blends [19]. SEM microphotographs show that the interfacial adhesion in the PE/COC blends is quite high because fracture surfaces pass through the COC particles rather than along the adjacent interface. This finding is supported by the fact that some links (probably thin fibers) between HDPE and COC can be observed at the interface. Nevertheless, the blend morphology on SEM microphotographs is somewhat unclear because of PE plastic deformations. For this reason, STEM microphotographs of RuO_4-stained ultrathin sections were taken (Fig. 3).

Figures 2 and 3 concurrently show the development of the co-continuous morphology in the PE/COC blend. The 85/15 blend consists of PE matrix and spherical or ellipsoidal COC particles whose average diameter is about 0.25 μm (diameter range: 0.1–0.4 μm). In the 70/30 blend, the average diameter is about 0.55 μm (diameter range: 0.1–1 μm), but some particles are elongated or irregular-shaped, which suggests that the COC particles coalesce and the structure tends to change to partially co-continuous. In the 50/50 blend, phase structure coarsening and co-continuity of the components are evident.

Crystallinity of a blend constituent may differ from that of the starting polymer due to interaction (partial miscibil-

15482634, 2005, 6, Downloaded from https://4spepublications.onlinelibrary.wiley.com/doi/10.1002/pen.20337 by Universita Di Trento, Wiley Online Library on [14/10/2026]. See the Terms and Conditions (https://onlinelibrary.wiley.com/terms-and-conditions) on Wiley Online Library for rules of use; OA articles are governed by the applicable Creative Commons License

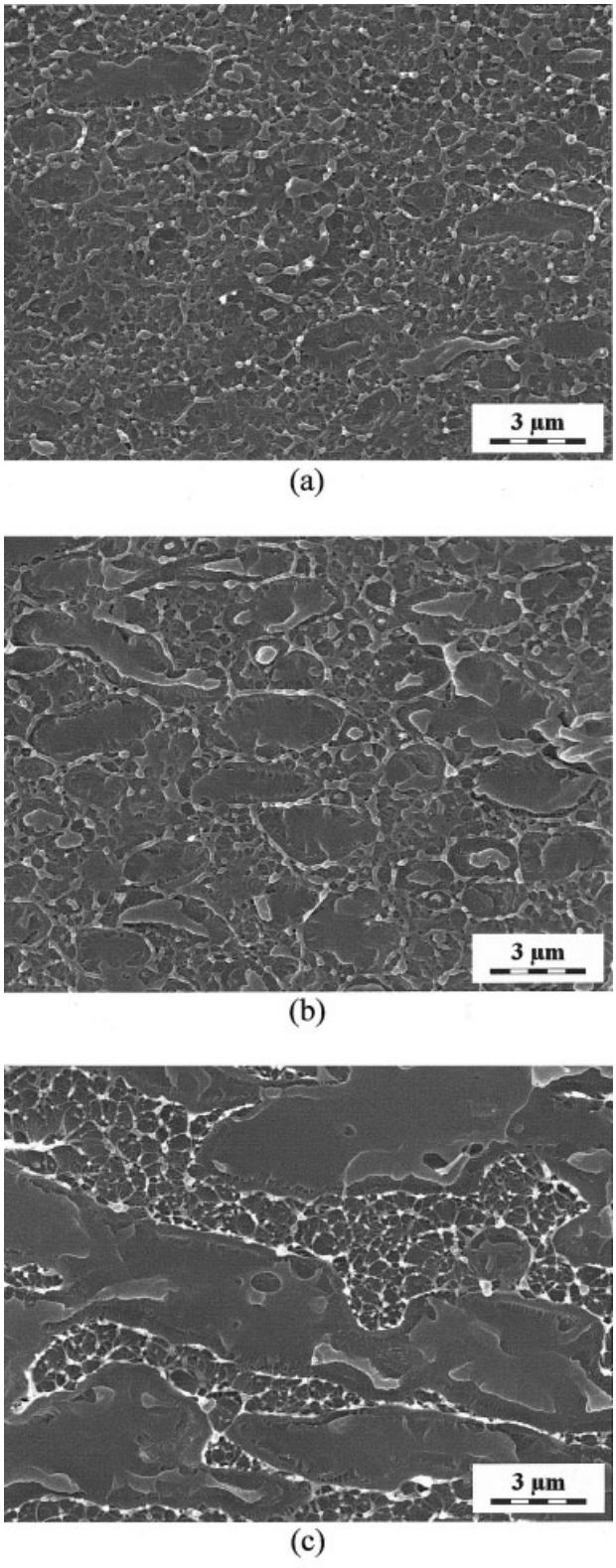


FIG. 2. SEM microphotographs of the phase structure of the HDPE/COC blends. (a) 85/15; (b) 70/30; (c) 50/50.

ity, nucleation activity) of the constituents. DSC measurements (Table 1) reveal that the HDPE component in the blends exhibits a slightly lower melting temperature T_m = 134−131°C (in both heating scans) than neat HDPE. Figure 4 shows that the melting enthalpy of HDPE in blends is not linearly proportional to its weight fraction, but is somewhat lower, which is more typical of as-molded blends [45–47].

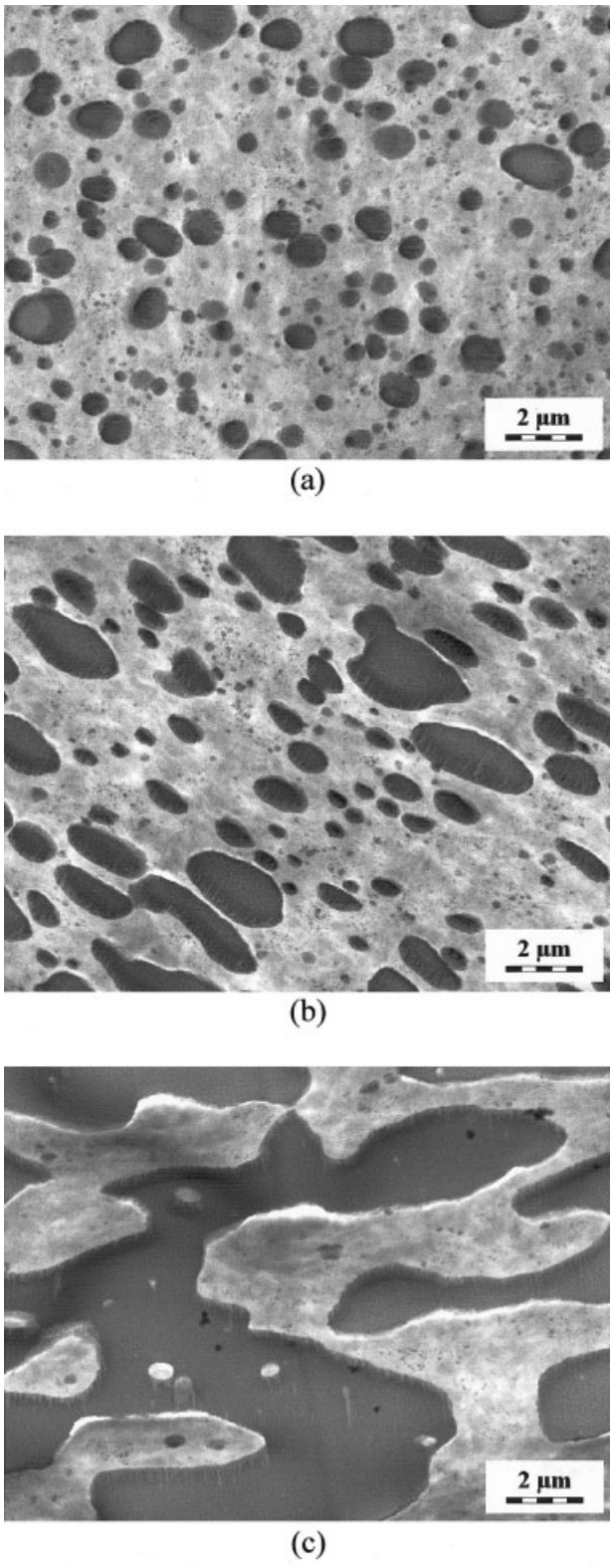


FIG. 3. STEM microphotographs of the phase structure of the HDPE/COC blends. (a) 85/15; (b) 70/30; (c) 50/50.

15482634, 2005, 6, Downloaded from https://4spepublications.onlinelibrary.wiley.com/doi/10.1002/pen.20337 by Universita Di Trento, Wiley Online Library on [14/10/2026]. See the Terms and Conditions (https://onlinelibrary.wiley.com/terms-and-conditions) on Wiley Online Library for rules of use; OA articles are governed by the applicable Creative Commons License

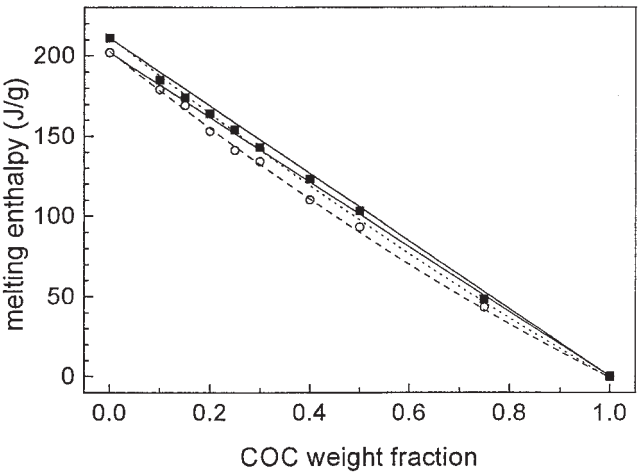


FIG. 4. Melting enthalpy of the HDPE component in HDPE/COC blends. Experimental data: first heating scan (○); second heating scan (■). Parameters of *Eq. 8b*: first heating scan (dashed line): $P_1 = 0.22$, $\Delta H_{m1} = 202$ J/g; second heating scan (dotted line): $P_1 = 0.10$, $\Delta H_{m1} = 211$ J/g; full lines: additivity.

Experimental data for blends consisting of two crystalline polymers can be fitted [48] by the empirical equation:

$$\Delta H_{mb} = \Delta H_{m1} w_1 (1 - P_1 w_2) + \Delta H_{m2} w_2 (1 - P_2 w_1) \qquad (8a)$$

where w_1 and w_2 are the weight fractions, ΔH_{m1} and ΔH_{m2} are the melting enthalpies of the neat components, and P_1 or P_2 are empirical parameters expressing a negative effect of component 2 on crystallinity of component 1 and vice versa.

As COC does not crystallize, *Eq. 8a* can be simplified for the HDPE/COC blends:

$$\Delta H_{mb} = \Delta H_{m1} w_1 (1 - P_1 w_2). \qquad (8b)$$

The value of $P_1 = 0.22$ was obtained for the first heating scan performed with as-molded specimens characterized by $\Delta H_{m1} = 202$ J/g for HDPE. These data are in good conformity with the negative deviation of density from linearity (additivity) as reported in Table 1. Moreover, ΔH_{mb} registered in the second heating scan shows a dependence on blend composition closer to linearity, i.e., $P_1 = 0.10$ ($\Delta H_{m1} = 211$ J/g), but the observed values are noticeably higher than those in the first scan. Crystallinity of the HDPE component in as-molded blends decreases proportionally to its weight fraction from approximately 69% for the neat HDPE to approximately 59% for the 25/75 blend. In the second heating scan, the crystallinity of HDPE component in the HDPE-rich blends ($w \geq 0.5$) is almost constant (about 70%) and only slightly lower than that of neat HDPE (72%). Higher values of crystallinity found in the second heating scan can be ascribed to more favorable conditions of crystallization (between the first and second heating scan) in comparison with those of as-molded specimens. It is worth noting that the crystallinity of HDPE in the 25/75 blend achieves lower values in both scans. The crystallization temperature T_{c1} of HDPE in blends seems to be 1–2°C higher than that of neat HDPE, which might indicate a tiny nucleating effect of COC.

TABLE 1. DSC data of the HDPE/COC blends as functions of composition.

				1st heating			Cooling		2nd heating		
HDPE/COC[a]	Density[b] (g/cm^3)	Difference[c] (%)	T_{g2}[d] (°C)	T_{g2}[e] (°C)	T_{m1}[f] (°C)	C_1[g] (%)	T_c[h] (°C)	C_1[i] (%)	T_{g2}[e] (°C)	T_{m1}[f] (°C)	C_1[g] (%)
100/0	0.956	0.00	–	–	135	68.8	112	71.6	–	134	71.9
90/10	0.960	–0.19	80	80	133	67.8	114	70.0	n.d.[j]	132	70.0
85/15	0.961	–0.38	78	79	134	67.7	114	69.3	77	132	69.7
80/20	0.963	–0.48	78	79	132	65.2	114	69.8	77	132	69.8
75/25	0.969	–0.15	78	79	134	64.1	114	70.0	76	132	70.0
70/30	0.971	–0.25	78	78	133	65.2	113	70.6	76	133	71.1
60/40	0.977	–0.22	79	79	134	62.5	113	69.3	77	132	69.8
50/50	0.981	–0.41	79	76	132	63.4	114	69.5	76	132	70.2
25/75	0.994	–0.55	80	79	131	58.6	114	63.5	78	131	63.3
0/100	1.014	0.00	81	81	–	–	–	–	80	–	–

[a] Blend composition in weight %.
[b] Density of as molded samples measured at 23°C in a helium pycnometer (standard deviation ±0.001 g/cm^3).
[c] Deviation from linearity in %.
[d] Glass transition temperature of COC measured at the maximum of loss modulus by DMTA.
[e] Glass transition temperature of COC detected by DSC.
[f] Melting temperature of HDPE component.
[g] Normalized crystallinity measured in the first or second heating.
[h] Crystallization temperature of HDPE component in the cooling scan.
[i] Normalized crystallization during the cooling scan.
[j] Not detectable.

15482634, 2005, 6, Downloaded from https://4spepublications.onlinelibrary.wiley.com/doi/10.1002/pen.20337 by Universita Di Trento, Wiley Online Library on [14/10/2026]. See the Terms and Conditions (https://onlinelibrary.wiley.com/terms-and-conditions) on Wiley Online Library for rules of use; OA articles are governed by the applicable Creative Commons License

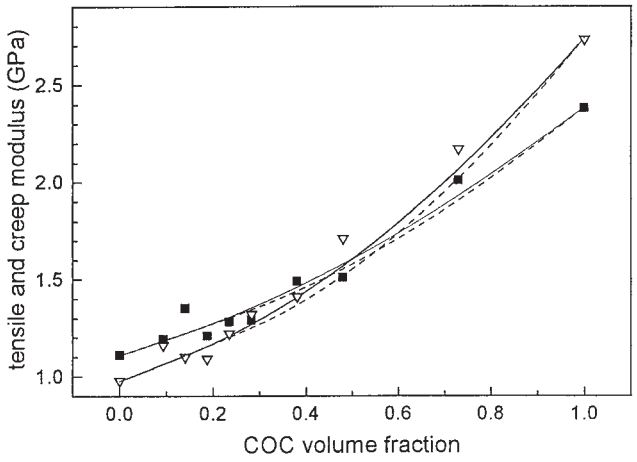


FIG. 5. Effect of the composition of HDPE/COC blends on tensile modulus E_b (■) and creep modulus E_{bc} (▽) at 23°C. Prediction of *Eq. 2* for "universal" input data $v_{1cr} = v_{2cr} = 0.16$ and $q = 1.8$ (full lines); adjusted parameters: $v_{1cr} = 0.16$, $v_{2cr} = 0.30$ and $q = 1.8$ (dashed lines).

Moduli of Blends

In general, microphotographs provide valuable information on the phase structure of blends; nonetheless, it is difficult to estimate the critical volume fraction of components. With regard to the percolation concept [39−41], it can be expected that physical properties of blends indicate the percolation threshold as a function of blend composition before the phase co-continuity is revealed by microphotographs. For this reason, it is useful to analyze the effect of blend composition on measured mechanical properties with the aid of the outlined predictive format.

Figure 5 documents that tensile modulus E_b and creep modulus E_{bc} of blends are reasonably fitted by *Eq. 2* with "universal" values $v_{1cr} = v_{2cr} = 0.16$ and $q = 1.8$. While v_{2cr} is certainly close to 0.16, the value of v_{1cr} is rather uncertain because the contribution of HDPE to blend mechanical properties is overshadowed by that of COC, which makes the format less sensitive to v_{1cr}. If $v_{2cr} = 0.30$ is assumed in conformity with STEM, the fitting of experimental data by *Eq. 2* is visibly worsened. The steeper increase in E_{bc} with the COC fraction—in comparison with that of E_b—can be ascribed to a different mode of testing. While the strain rate in stress-strain measurements was identical for all blend species, in creep measurements the strain rate of creeping markedly diminished with the COC fraction in blends.

Dynamic mechanical patterns (Fig. 6) of the HDPE/COC blends taken in the interval from −140 to 120°C display three loss modulus peaks. The γ-peak at about −105°C corresponds to local molecular mobility in the noncrystalline regions of HDPE. COC displays an analogous relaxation at a lower temperature, approximately –120°C, than HDPE, which can be explained by relatively higher mobility of ethylene sequences in the totally amorphous copolymer. In the HDPE/COC blends, both intensity and temperature of the γ-peak decrease with the COC fraction. The α-relaxation peak of HDPE at about 45°C is associated with some type of molecular motions in crystals and interfacial regions of lamellae [49−51]. The 80°C peak obviously corresponds to glass (α) transition of COC [6, 14], because it is accompanied by a steep drop of the storage modulus. Its temperature location is in a good conformity with DSC measurements indicating $T_{g2} = 81$°C for neat COC and about 78−79°C for the COC component in blends (Table 1), which might evidence a very limited miscibility of COC and HDPE. Figure 6 also shows that storage modulus in the range 0–70°C increases with the percentage of COC in blends, which evidences the stiffening effect of COC.

Calculated dependencies of E′ and E″ on blend composition are confronted in Fig. 7 with experimental data read off for –50, 23, and 100°C. Such graphs are also instructive from the viewpoint of conceivable applications of the HDPE/COC blends. While E′(−50°C) and E′(23°C) do not noticeably change with the blend composition, E′(100°C) markedly decreases with the COC fraction, which means that COC has a detrimental effect on dimensional stability

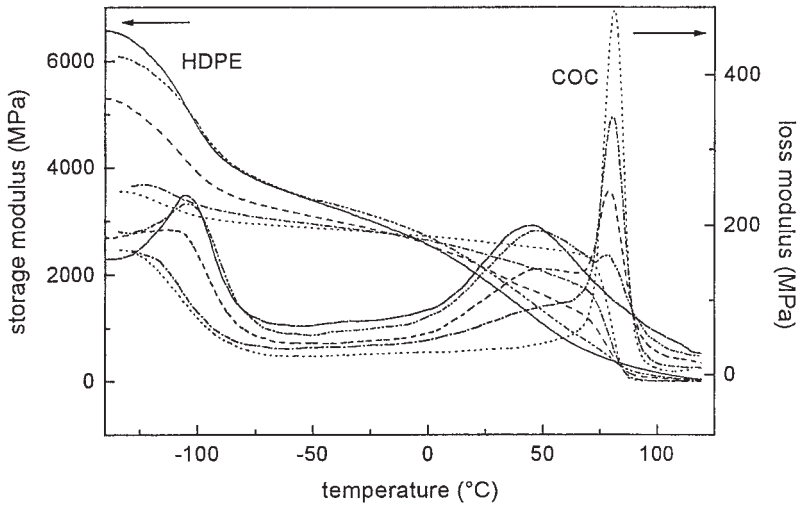


FIG. 6. Effect of the composition of HDPE/COC blends on the temperature dependence of the storage modulus E_b' and of the loss modulus E_b''. HDPE/COC = 100/0 (full line); 75/25 (dash-dot-dot line); 50/50 (dashed line); 25/75 (dash-and-dot line); 0/100 (dotted line).

15482634, 2005, 6, Downloaded from https://4spepublications.onlinelibrary.wiley.com/doi/10.1002/pen.20337 by Universita Di Trento, Wiley Online Library on [14/10/2026]. See the Terms and Conditions (https://onlinelibrary.wiley.com/terms-and-conditions) on Wiley Online Library for rules of use; OA articles are governed by the applicable Creative Commons License

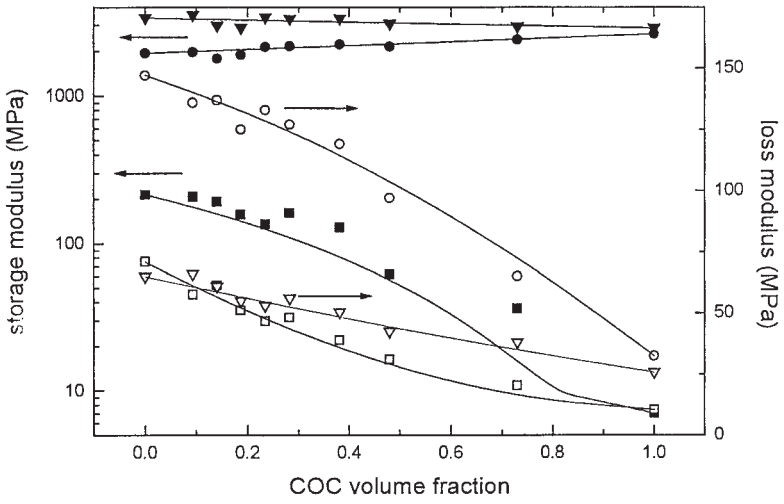


FIG. 7. Effect of the composition of HDPE/COC blends on storage modulus E_b' (full points) and loss modulus E_b'' (empty points) read at –50°C (triangles), 23°C (circles) or 100°C (squares). Prediction of *Eqs. 3* and *4* for "universal" input data $v_{1cr} = v_{2cr} = 0.16$ and $q = 1.8$ (full lines).

of the blends at temperatures above 80°C. As can be seen, experimental data are plausibly fitted by *Eqs. 3* and *4* with "universal" values $v_{1cr} = v_{2cr} = 0.16$ and $q = 1.8$.

Coefficient of Thermal Expansion

The coefficient of (linear) thermal expansion was evaluated for three temperature intervals between –10 and 70°C as indicated in Fig. 8. The value of CTE for neat HDPE increases with temperature from 0.90×10^{-4} K^{-1}at 0°C to 2.20×10^{-4} K^{-1} at 55°C, while COC is characterized by values 0.65×10^{-4} K^{-1} and 1.1×10^{-4} K^{-1}. These data are in a good agreement with the values reported in literature, i.e., $1.00–1.50 \times 10^{-4}$ K^{-1} for PE [52] and 0.70×10^{-4} K^{-1} for COC [53]. CTE found for the temperature intervals from –10 to 10°C and from 10 to 40°C are almost independent of blend composition in the interval $0 < v_2 < 0.3$, thus indicating the dominating effect of the HDPE component. For $v_2 > 0.3$, a virtually linear decrease in CTE with the COC fraction indicates increasing co-continuity and the role of the COC component. In the temperature interval from 40 to 70°C, which is located above the α-transition of HDPE, an almost constant CTE was found for blends with $0.10 \leq v_2 \leq 0.50$. A higher value found for the 25/75 blend may be associated with lower crystallinity of HDPE in this blend.

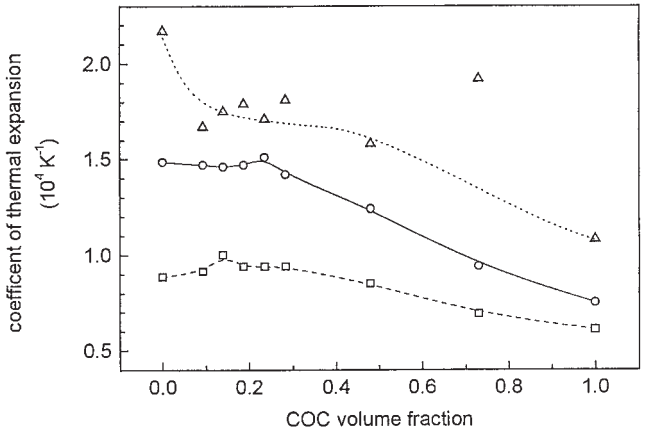


FIG. 8. Coefficient of linear thermal expansion as a function of the HDPE/COC blend composition. Temperature range of reading: −10 to 10°C (□); 10 to 40°C (○); 40 to 70°C (△).

Strength of Blends

Inspecting Fig. 9, we can see that experimental data for yield or tensile strength are reasonably fitted by *Eq. 6* with "universal" values $v_{1cr} = v_{2cr} = 0.16$, $q = 1.8$ and $A = 1$. Similarly to Fig. 5, the fitting becomes poorer if $v_{2cr} = 0.30$ is assumed. Obviously, as soon as the COC component assumes partial continuity, the term $S_{y2}v_{2p}$ in *Eq. 6* accounts for a pronounced increase in S_{yb} because $S_{y2} \approx 3\ S_{y1}$. Also experimental data on tensile strength S_{ub} of blends approximately follow—except for the value found for the 25/75 blend—the dependence predicted by *Eq. 6*, which corroborates the applicability of the format.

As can clearly be seen in Fig. 9b, strain at break decreases by two orders of magnitude throughout the composition range; its profound drop in the region around $v_2 = 0.2$ is another manifestation of the formation of co-continuous brittle component of COC. On the other hand, yield strain displays (Fig. 9a) a monotonic decrease with v_2 from 8.7% for PE to approximately 2% for COC without exhibiting any "break" at v_{2cr}. Tensile energy to break and tensile impact strength (Fig. 10) show a conspicuous drop in the interval $0.10 < v_2 \leq 0.30$, which evidences the detrimental effect of COC on the blend toughness. (We can only speculate that a markedly lower value of tensile energy to break for the 85/15 blend is a consequence of nonidentified latent defects in the used test specimens.) Further growth of COC fraction accounts for further deterioration of blend properties to the values typical of brittle polymers. However, tensile impact strength shows a local maximum at HDPE/COC = 25/75, which probably corresponds to COC toughened with HDPE particles [54]. Ultimate mechanical properties of blends cannot be treated in terms of the EBM so that there is no

15482634, 2005, 6, Downloaded from https://4spepublications.onlinelibrary.wiley.com/doi/10.1002/pen.20337 by Universita Di Trento, Wiley Online Library on [14/10/2026]. See the Terms and Conditions (https://onlinelibrary.wiley.com/terms-and-conditions) on Wiley Online Library for rules of use; OA articles are governed by the applicable Creative Commons License

comparison possible between experimental and theoretical data.

CONCLUSIONS

Experimental data for tensile modulus E_b, creep modulus E_{crb}, storage modulus E_b', loss modulus E_b'', yield strength S_{yb}, and tensile strength S_{ub} are reasonably fitted by *Eqs. 2*, *3*, *4*, *6*, and *7* of the predictive format for $v_{1cr} = v_{2cr} = 0.16$ and $q = 1.8$. The applicability of the predictive format is enabled by the fact that the crystallinity of HDPE is virtually independent of blend composition. In conformity with the percolation concept, mechanical properties of blends reveal the percolation threshold of COC at a lower fraction than microphotographs. The value of v_{1cr} remains somewhat uncertain because the contribution of COC to blend mechanical properties overshadows that of HDPE and makes the format less sensitive to v_{1cr}. The dependencies of

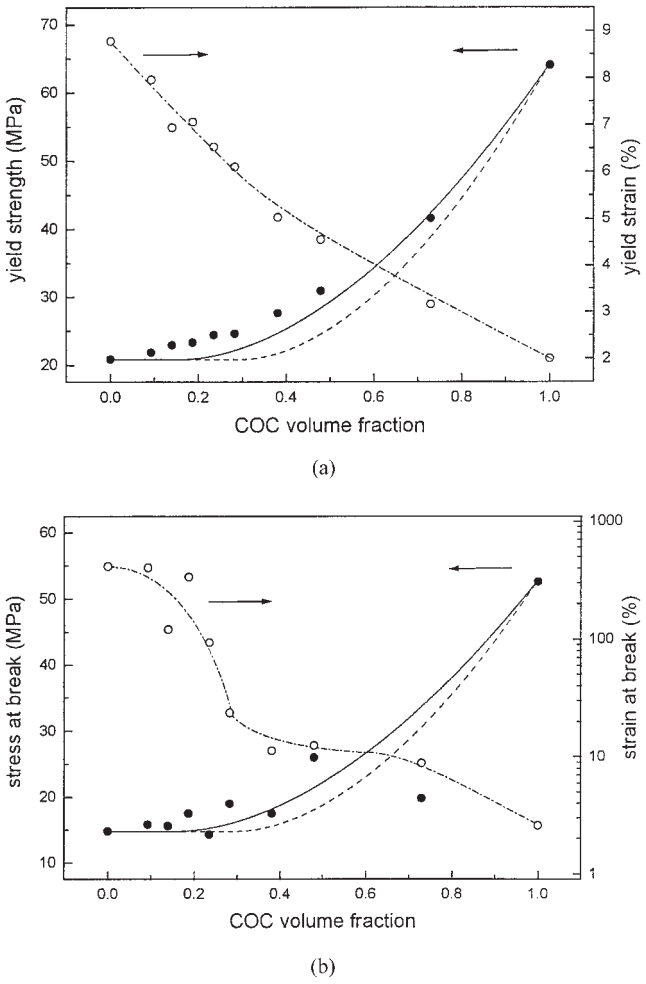


FIG. 9. Effect of the composition of HDPE/COC blends on (a) yield strength and yield strain and (b) stress at break and strain at break. Prediction of *Eq. 6* for "universal" input data $v_{1cr} = v_{2cr} = 0.16$ and $q = 1.8$ (full lines); adjusted parameters: $v_{1cr} = 0.16$, $v_{2cr} = 0.30$ and $q = 1.8$ (dashed lines); experimental data of yield strain or strain at break (dash-and-dot lines).

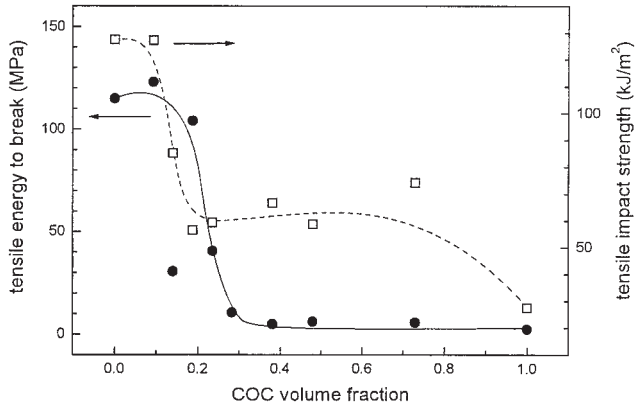


FIG. 10. Effect of the composition of HDPE/COC blends on their tensile energy to break (●) and tensile impact strength (□). No predicted dependencies.

S_{yb} and S_{ub} on blend composition indicate that interfacial adhesion in the PE/COC blends is strong enough to transmit acting stress up to the break point. Strain at break, tensile energy to break and tensile impact strength show profound drops in the region around $0.15 < v_2 < 0.25$, which corroborates the beginning of the formation of co-continuous brittle component of COC. Further growth of COC fraction accounts for their reduction to the values typical of brittle polymers; however, tensile impact strength shows a local maximum at HDPE/COC = 25/75, which can be ascribed to toughening of COC with HDPE particles.

ACKNOWLEDGMENTS

J.K. and M.Š. are indebted to the Grant Agency of the Czech Republic for financial support of this research through grants 106/04/1051 (to J.K.) and 106/02/P029 (to M.Š.). We thank D. Michálková (for preparation of blends and measurements of tensile impact strength) and L. Kaprálková (for Instron Tester measurements) for their assistance.

REFERENCES

1. L.A. Utracki, *Polymer Alloys and Blends*, Hanser, Munich (1990).
2. M.J. Folkes and P.S. Hope, *Polymer Blends and Alloys*, Chapman & Hall, Cambridge (1993).
3. L.H. Sperling, *Polymeric Multicomponent Materials*, Wiley, New York (1997).
4. L.A. Utracki, *Commercial Polymer Blends*, Chapman & Hall, London (1988).
5. D.R. Paul and C.B. Bucknall, eds., *Polymer Blends*, Wiley, New York (1999).
6. D. McNally, in *Encyclopedia of Polymer Science and Technology*, Vol. 2, 3rd ed., H.F. Mark, ed., Wiley, Hoboken, NJ, 489 (2003).
7. K. Thorshaug, R. Mendichi, L. Boggioni, I. Tritto, S. Trinkle,

15482634, 2005, 6, Downloaded from https://4spepublications.onlinelibrary.wiley.com/doi/10.1002/pen.20337 by Universita Di Trento, Wiley Online Library on [14/10/2026]. See the Terms and Conditions (https://onlinelibrary.wiley.com/terms-and-conditions) on Wiley Online Library for rules of use; OA articles are governed by the applicable Creative Commons License

C. Friedrich, and R. Muelhaupt, *Macromolecules*, **35**, 2903 (2002).
8. L. Tritto, L. Boggioni, J.C. Jansen, K. Thorshaug, M.C. Sacchi, and D.R. Ferro, *Macromolecules*, **35**, 616 (2002).
9. G. Khanarian, *Polym. Eng. Sci.*, **40**, 2590 (2000)**.**
10. W.J. Huang, F.C. Chang, and P.P.J. Chu, *Polymer*, **41**, 6095 (2000).
11. P.P.J. Chu, W.J. Huang, and F.C. Chang, *Polymer*, **42**, 2185 (2001).
12. T. Scrivani, R. Benavente, E. Perez, and J.M. Perena, *Macromol. Chem. Phys.*, **202**, 2547 (2001).
13. J. Forsyth, J.M. Perena, R. Benavente, E. Perez, I. Tritto, L. Boggioni, and H.H. Brintzinnger, *Macromol. Chem. Phys.*, **202**, 614 (2001).
14. J.F. Forsyth, T. Scrivani, R. Benavente, C. Marestin, and J.M. Perena, *J. Appl. Polym. Sci.*, **82**, 2159 (2001).
15. D. Rana, C.H. Lee, K. Cho, B.H. Lee, and S. Choe, *J. Appl. Polym. Sci.*, **69**, 2441 (1998).
16. J. Luettmer-Strathmann and J.E.G. Lipson, *Macromolecules*, **32**, 1093 (1999).
17. A. Pegoretti, J. Kolařík, L. Fambri, and A. Penati, *Polymer*, **44**, 3381 (2003).
18. J. Kolařík, A. Pegoretti, L. Fambri, and A. Penati, *Macromol. Mater. Eng.*, **288**, 629 (2003).
19. M. Šlouf, J. Kolařík, and L. Fambri, *J. Appl. Polym. Sci.*, **91**, 253 (2004).
20. T. Matsuoka and S. Yamamoto, *J. Appl. Polym. Sci.*, **68**, 807 (1998).
21. R.C. Willemse, A.P. de Boer, J. Van Dam, and A.D. Gotsis, *Polymer*, **39**, 5879 (1998).
22. R.C. Willemse, *Polymer*, **40**, 2175 (1999).
23. H. Veenstra, J. Van Dam, and A.P. De Boer, *Polymer*, **40**, 1190 (1999).
24. H. Veenstra, P.C.J. Verkooijen, B.B.J. van Lent, J. Van Dam, A.P. De Boer, and H.J. Nijhof, *Polymer*, **41**, 1817 (2000).
25. L.E. Nielsen and R.F. Landel, *Mechanical Properties of Polymers and Composites*, Marcel Dekker, New York (1994).
26. J. Lyngaae-Jorgensen, A. Kuta, K. Sondergaard, and K.V. Poulsen, *Polym. Networks*, **3**, 1 (1993).
27. J. Kolařík and G. Geuskens, *Polym. Networks Blends*, **7**, 13 (1997).
28. H. Veenstra, J. van Dam, and A.P. de Boer, *Polymer*, **40**, 1119 (1999).
29. J. Kolařík, L. Fambri, A. Pegoretti, A. Penati, *Polym. Eng. Sci*., **40**, 127 (2000).
30. J. Lyngaae-Jorgensen, K.L. Rasmussen, E.A. Chtcherbakova, and L.A. Utracki, *Polym. Eng. Sci.*, **39**, 1060 (1999).
31. J. Lyngaae-Jorgensen and L.A. Utracki, *Polymer*, **44**, 1661 (2003).
32. J. Kolařík, A. Pegoretti, L. Fambri, and A. Penati, *J. Polym. Res*., **7**, 1 (2000).
33. J. Kolařík, *Eur. Polym. J.*, **34**, 585 (1998).
34. J. Kolařík, *J. Macromol. Sci., Phys.*, **39**, 53 (2000).
35. J. Kolařík, L. Fambri, A. Pegoretti, and A. Penati, *Polym. Adv. Technol*., **11**, 75 (2000).
36. J. Kolařík, L. Fambri, A. Pegoretti, A. Penati, and P. Goberti, *Polym. Eng. Sci*., **42**, 161 (2002).
37. G.M. Brown and J.H. Butler, *Polymer*, **38**, 3937 (1997).
38. B. Wunderlich and G. Czornyj, *Macromolecules*, **10**, 906 (1977).
39. P.G. De Gennes, *J. Phys. Lett. (Paris)*, **37**, L1 (1976).
40. J. Sax and J.M. Ottino, *Polym. Eng. Sci*., **23**, 165 (1983).
41. W.Y. Hsu and S. Wu, *Polym. Eng. Sci.*, **33**, 293 (1993).
42. R.M. Christensen, *Mechanics of Composite Materials*, Wiley, New York (1979).
43. J. Kolařík, *Polym. Eng. Sci*., **36**, 2518 (1996).
44. P.G. Fox and K.N.G. Fuller, *Nat. Phys. Sci.*, **234**, 13 (1971).
45. M. Shibata, R. Yosomiya, Z. Jiang, Z. Yang, G. Wang, R. Ma, and Z. Wu, *J. Appl. Polym. Sci.*, **74**, 1686 (1999).
46. L. Minkova, H. Yordanov, and S. Filippi, *Polymer*, **43**, 6195 (2002).
47. G. Guerra, C. De Rosa, V.M. Vitagliano, V. Petraccone, P. Corradini, *J. Polym. Sci. B: Polym. Phys.*, **29**, 265 (1991).
48. J. Kolařík, L. Fambri, M. Šlouf, and D. Konečný, *J. Appl. Polym. Sci*., in press.
49. Y.P. Khanna, E.A. Turi, T.J. Taylor, V.V. Vickroy, and R. F. Abbott, *Macromolecules*, **18**, 1302 (1985).
50. P. Starck, *Eur. Polym. J.*, **33**, 339 (1997).
51. H. Sha, X. Zhang, and I.R. Harrison, *Thermochimica Acta*, **192**, 233 (1991).
52. E. Benham and M. Mc Daniel, in *Encyclopedia of Polymer Science and Technology*, Vol. 2, 3rd ed., H.F. Mark, ed., Wiley, Hoboken, NJ, 392 (2003).
53. Topas (COC), brochure from Ticona, Hoechst, Germany (1995).
54. G. Khanarian, *Polym. Eng. Sci.*, **40**, 2590 (2000).

15482634, 2005, 6, Downloaded from https://4spepublications.onlinelibrary.wiley.com/doi/10.1002/pen.20337 by Universita Di Trento, Wiley Online Library on [14/10/2026]. See the Terms and Conditions (https://onlinelibrary.wiley.com/terms-and-conditions) on Wiley Online Library for rules of use; OA articles are governed by the applicable Creative Commons License